Eddy-wind interactions stimulate extraordinary mid-ocean plankton blooms

One-sentence summary: Mid-ocean eddies, together with wind-forced motions, cause episodic bursts of nutrient supply to the upper ocean, changes in plankton community structure, and export of organic material to the deep sea.

Dennis J. McGillicuddy, Jr.[1*], Laurence A. Anderson[1], Nicholas R. Bates[2], Thomas Bibby[3,4], Ken O. Buesseler[1], Craig Carlson[5], Cabell S. Davis[1], Courtney Ewart[5], Paul G. Falkowski[3], Sarah A. Goldthwait[6,7], Dennis A. Hansell[8], William J. Jenkins[1], Rodney Johnson[2], Valery K. Kosnyrev[1], James R. Ledwell[1], Qian P. Li[8], David A. Siegel[5], Deborah K. Steinberg[6]

Manuscript revised and resubmitted to *Science*
January 29, 2007

[1]Woods Hole Oceanographic Institution, Woods Hole, MA 02543-1541, USA.

[2]Bermuda Institute of Ocean Sciences, Ferry Reach, GE01, Bermuda.

[3]Institute of Marine and Coastal Sciences, Rutgers University, New Brunswick, NJ 08901-8521, USA.

[4]School of Ocean and Earth Science, National Oceanography Centre, University of Southampton, Southampton SO14 3ZH, United Kingdom.

[5]University of California, Santa Barbara CA 93106, USA.

[6]Virginia Institute of Marine Science, Gloucester Pt., VA 23062-1346, USA.

[7]Humboldt State University, Arcata, CA 95521, USA.

[8]Rosenstiel School of Marine and Atmospheric Science, University of Miami, Miami, FL 33149, USA.

*To whom correspondence should be addressed. Email: dmcgillicuddy@whoi.edu

Episodic eddy-driven upwelling may supply a significant fraction of the nutrients required to sustain primary productivity of the subtropical ocean. New observations in the northwest Atlantic reveal that, although plankton blooms occur in both cyclones and mode-water eddies, the biological responses differ. Mode-water eddies can generate extraordinary diatom biomass and primary production at depth, relative to the time-series near Bermuda. These blooms are sustained by eddy-wind interactions, which amplify the eddy-induced upwelling. In contrast, eddy-wind interactions dampen eddy-induced upwelling in cyclones. Carbon export inferred from oxygen anomalies in eddy cores is 1-3 times annual new production for the region.

Understanding the controls on primary production in the upper ocean is of fundamental importance for two main reasons. First, primary productivity sets a first-order constraint on the energy available to sustain oceanic ecosystems. Second, fixation and subsequent sinking of organic particles removes carbon from the surface ocean (the so-called "biological pump"), which plays a key role in partitioning of carbon dioxide between the ocean and atmosphere. Geochemical estimates of new production (*1*) surpass the apparent rate of nutrient supply by vertical mixing by a factor of two or more in subtropical oceans (*2-6*), which constitute some of the largest biomes on earth. Two possible mechanisms to supply the "missing" nutrient locally include nitrogen fixation by cyanobacteria (*7-10*), and intermittent upwelling by mesoscale eddies and submesoscale processes (*11-21*).

There are at least three types of mid-ocean eddies in the northwestern subtropical Atlantic: cyclones, anticyclones, and mode-water eddies (Fig. 1A). Cyclones dome both the seasonal and main pycnoclines, whereas regular anticyclones depress both density interfaces. Mode-water eddies derive their name from the thick lens of water that deepens the main pycnocline while shoaling the seasonal pycnocline. Because the geostrophic velocities are dominated by depression of the main pycnocline, the direction of rotation in mode-water eddies is the same as regular anticyclones. However, displacement of the seasonal pycnocline is the same as in cyclones: both types of features tend to upwell nutrients into the euphotic zone during their formation and intensification phases. As these eddies spin down, the density surfaces relax back to their mean positions, and thus decaying cyclones and mode-water eddies will have downwelling in their interiors. This temporal evolution during the life cycle of an eddy is a key regulator of the biogeochemical response (*22*, *23*).

Eddy features are readily discernible via satellite altimetry (Fig. 1B; fig. S1). Access to these data in near real-time (*24*) facilitates tracking of individual eddies and adaptive sampling in shipboard operations. In 2004 and 2005 we sampled a total of ten different eddies, five more than once (Table S1). Time-series within target features allows resolution of temporal dynamics in eddy-driven nutrient supply, phytoplankton physiological response, changes in community structure, and biogeochemical fluxes. We focus this discussion on cyclone "C1" and mode-water eddy "A4"; findings in other cyclones and mode-water eddies in this study (Table S1) as well as prior investigations (Table S2) are consistent with that presented herein.

Cyclone C1 was occupied four times between June and August 2004 (*25*). Shipboard acoustic Doppler current profiler (ADCP) data documented the counterclockwise flow associated with C1's negative sea level anomaly (SLA), and its altimetric history suggested intensification in May. Uplift of near-surface isopycnals was associated with shoaling and enhancement of the subsurface chlorophyll maximum. The magnitude of the subsurface chlorophyll maximum in C1 was lower than other cyclones (Fig. 2A), yet still in the upper quartile of all subsurface maxima observed in the Bermuda Atlantic Time-series Study (BATS) (*26*) 1988-2003.

Phytoplankton species composition in cyclone C1 resembled mean conditions at BATS (Fig. 2B). On average, *Prochlorococcus* spp., *Synechococcus* spp., pelagophytes, and prymnesiophytes constitute the largest fractions of total chlorophyll *a* in the 75-140m depth interval (deep chlorophyll maximum) at BATS; diatoms, dinoflagellates, and prasinophytes contribute comparatively little to total chlorophyll *a*. The eddy-induced bloom in C1 increased the relative amount of *Prochlorococcus* spp., decreased the relative amount of *Synechococcus* spp., and the rare groups became an even smaller fraction of total chlorophyll *a*.

In subsequent occupations of cyclone C1, conditions at eddy center changed from a local maximum to a local minimum in chlorophyll *a* and fluorescence. During this latter phase, integrated primary production at eddy center was not statistically distinguishable from climatological summertime conditions at BATS, nor were bacterial production and biomass (Table S3). However, systematic mesoscale variability was observed in microbial parameters, with biomass and production enhancement at the periphery relative

to eddy center. Zooplankton biomass was also elevated on the periphery relative to eddy center, with large zooplankton migrators (>5mm) increasing most. Although zooplankton biomass was not significantly different from the long-term BATS summertime mean (1994-2005), there was significant enhancement (ANOVA, $P<0.05$) above mean summertime conditions for 2004-2005 (Table S3).

Export measured with drifting sediment traps was below the BATS summertime mean, although not anomalously so given the variability at BATS (Table S3). ^{234}Thorium-based export fluxes were consistent with these findings (Table S3). However, subsurface oxygen distributions suggest a significant export event prior to our observations. During the first occupation, cyclone C1 contained an oxygen minimum in the 200-400m depth interval (*27*) in which the oxygen concentrations were lower than all previous measurements at BATS in that stratum (Fig. 2C). Nitrate and dissolved inorganic carbon were also enhanced in the feature, in approximately Redfield proportion with the oxygen anomaly. One month later, the magnitude of the oxygen anomaly had decreased by 50% (Fig 2C). Thus, the oxygen deficit appears to be an ephemeral feature with a time scale shorter than the lifetime of the eddy.

An estimate of remineralization implied by the oxygen deficit can be computed from differences in oxygen inventories inside versus outside of the eddy in this depth interval (Fig. 2C) (*28*). Using photosynthetic stoichiometry of 138 O_2 : 106 C : 16 N : 1 P, remineralization is 1.4 mol N m^{-2}, approximately three times annual new production for the region (*3*). Water mass analysis suggests the eddy core may have had a distant origin in the southern Sargasso Sea. Using biogeochemical characteristics of the distant waters

as the background from which the anomaly is computed, the implied remineralization is 0.7±0.2 mol N m^{-2}, approximately 1.4 times annual new production at BATS.

Mode-water eddy "A4" was occupied six times between June and September 2005. Its sea level anomaly was positive (Fig. 1B), and shipboard ADCP measurements confirmed anticyclonic flow. Its altimetric history suggested a relatively persistent SLA of 20cm for the four months preceding our first occupation.

High-resolution surveys with a towed undulating Video Plankton Recorder (*29*) revealed an extraordinary phytoplankton bloom in the interior of A4 (Fig. 3A). Although submesoscale variability is evident, the enhancement spans the eddy's inner core (*30*). Peak chlorophyll *a* measured near eddy center was 1.4 μg Chl *a* l^{-1}, eclipsing the highest value ever measured at BATS by a considerable margin (Fig. 2A). This measurement is eight standard deviations above the mean subsurface maximum at BATS.

Phytoplankton species composition in mode-water eddy A4 departed dramatically from mean conditions at BATS (Fig. 2B), expressed primarily in a shift toward a diatom-dominated community (*31*). The amount of chlorophyll *a* in diatoms in A4 was 8 standard deviations above the BATS mean. Shipboard microscopic cell counts from a sample in the high chlorophyll region indicated ca. 8000 colonies l^{-1} of the chain-forming diatom *Chaetoceros* spp. Given that each colony contained ca. 15 cells, we estimate the diatom concentration to be 4-5 orders of magnitude above the background concentration of 1-10 cells l^{-1}. The propensity of mode-water eddies to form diatom blooms emerges as a systematic aspect of these data (Table S1) and prior observations (Table S2): the three highest chlorophyll *a* values in the present data, and two of the three highest values in the

BATS time series (*22, 32*) (Fig. 2A) were all associated with diatom-dominated phytoplankton communities in mode-water eddies (*33*).

In the first occupation of mode-water eddy A4, primary production was not significantly different from mean summertime conditions at BATS. In the second occupation, primary production was significantly enhanced (Table S3)(*34*). The primary production anomaly had an unusual vertical structure, with a subsurface maximum that exceeded the envelope of BATS observations in the 60-80m depth interval (Fig. 3B). This structure is consistent with enhanced nutrient supply from below and a diatom population capable of high growth rates in low light conditions (*35*)(*36*).

Zooplankton biomass at eddy center varied more than three-fold (Table S3). Maximum vertically-integrated biomass occurred at the same location as the anomalously high primary production (Fig. 3B), with the largest increase in the 1-5mm size range. Zooplankton biomass in A4 was higher than 2004-2005 BATS summer samples, but not significantly different (ANOVA, $P>0.05$) from the long-term BATS summer mean (Table S3). However, samples from cyclones and mode-water eddies comprise six of the top ten highest zooplankton biomass observations in the combined data set.

Export measured in A4 was below the BATS summertime mean, although within the range of variability observed at BATS (Table S3). ^{234}Thorium-based export flux estimates yielded similar values (Table S3). The bloom in A4 was accompanied by exceptionally low oxygen concentrations (ca. 120 μmol kg^{-1}) in the 800-1000m depth interval (Fig. 2D), lower than ever measured at BATS. Remineralization implied by the difference between the observed oxygen deficit inside the eddy and background

conditions outside the eddy is 0.8 mol N m^{-2} (*28*), ca. 1.6 times the annual new production for the region. As in cyclone C1, the oxygen deficit coincided with a discernible salinity anomaly, suggesting that the water mass may have had a distant origin. The climatological salinity distribution (*37*) indicates potential origins along the northern and southern limbs of the subtropical gyre. The latter contain oxygen concentrations comparable to that observed in the core of A4, whereas the former contain much more oxygen. Thus, the southern source region implies the oxygen deficit is primarily an advective feature, whereas the northern source region requires a substantial eddy-induced export event (*38*).

Why is the biological response to cyclones and mode-water eddies so different? Macronutrient stoichiometries just below the euphotic zone are similar (*39*), suggesting a physical cause. We hypothesize the difference arises from asymmetry in vertical motions induced by eddy-wind interactions. To quantify this effect, we used a model of uniform wind blowing over an idealized anticyclonic vortex, with wind stress formulated as the difference between air and water velocities at the sea surface (*40*). Stress is enhanced on the flank of the eddy where wind and current oppose each other, and stress is reduced on the flank where they flow in the same direction. This generates a divergence in the center of an anticyclone regardless of wind direction. Applying this model to A4, the upwelling velocity induced by the eddy-wind interaction ranges from 0.1 to 1.6 m d^{-1} (Fig. 4) (*41*). Upward motion in the interior of A4 was confirmed by a tracer release experiment, during which the tracer moved upward at 0.4 m d^{-1}, almost exactly the rate predicted from the eddy-wind interaction model (Fig. 4).

The eddy-wind interaction model predicts *downwelling* in the interior of cyclone C1 (Fig. 4). The low biomass and productivity at eddy center during the latter stages of our observations are consistent with the predicted eddy-wind induced downwelling. Unfortunately, there was no tracer release in C1 that can be used to test this prediction. Nevertheless, it is clear that eddy-wind interactions enhance the vertical nutrient flux in mode-water eddies, and counterbalance it in cyclones (Fig. 1A). This may explain why phytoplankton enhancement in cyclones is rather ephemeral, whereas mode-water eddies can produce long-lasting blooms of diatoms (*42*).

Observations presented herein document eddy-driven events that exceeded the envelope of variability in prior measurements of chlorophyll *a*, primary productivity at depth, and oxygen in a particularly well-studied region of the world ocean. Episodic phenomena continue to be undersampled in extant oceanographic databases, and the prospects for capturing them in traditional time-series mode are statistically humbling (*43*). More complete assessment of the influence of eddies on biogeochemical cycling will require models that fully resolve these processes. Existing models differ in this regard, some indicating little integrated impact (*44*) while others suggest that eddies are the dominant mechanism of nutrient supply in the interior of the subtropical gyre (*45*). Improved estimates will require a number of revisions to prior models so that different responses in cyclones and mode-water eddies can be resolved. These include explicit representation of eddy-wind interactions and mechanistic links between mesoscale dynamics, species composition, and export (*46*).

References and Notes

1. New production is that fraction of total production supported by exogenous nutrients, as per R. C. Dugdale, J. J. Goering, *Limnol. Oceanogr.* **12**, 196 (1967).
2. E. Schulenberger, J. L. Reid, *Deep-Sea Res.* **28A**, 901 (1981).
3. W. J. Jenkins, J. C. Goldman, *J. Mar. Res.* **43**, 465 (1985).
4. M. R. Lewis, W. G. Harrison, N. S. Oakley, D. Hebert, T. Platt, *Science* **234**, 870 (1986).
5. T. Platt, W. G. Harrison, *Nature* **318**, 55 (1985).
6. S. Emerson, S. Mecking, J. Abell, *Global Biogeochem. Cycles* **15**, 535 (2001).
7. D. G. Capone, J. P. Zehr, H. W. Pearl, B. Bergman, E. J. Carpenter, *Science* **276**, 1221 (1997).
8. D. Karl *et al.*, *Nature* **388**, 533 (1997).
9. N. Gruber, J. L. Sarmiento, *Global Biogeochem. Cycles* **11**, 235 (1997).
10. R. R. Hood, V. J. Coles, D. G. Capone, *J. Geophys. Res.* **109**, doi:10.1029/2002JC001753 (2004).
11. P. G. Falkowski, D. Ziemann, Z. Kolber, P. K. Bienfang, *Nature* **352**, 55 (1991).
12. D. J. McGillicuddy *et al.*, *Nature* **394**, 263 (1998).
13. A. Oschlies, V. C. Garcon, *Nature* **394**, 266 (1998).
14. A. Mahadevan, D. Archer, *J. Geophys. Res.* **105**, 1209 (2000).
15. M. Lévy, P. Klein, A.-M. Treguier, *J. Mar. Res.* **59**, 535 (2001).
16. J. D. Woods, in *Toward a Theory on Biological-Physical Interactions in the World Ocean* B. J. Rothschild, Ed. (D. Reidel, Dordrecht, 1988).

17. R. G. Williams, M. J. Follows, in *Ocean Biogeochemistry: The role of the ocean carbon cycle in global change* M. J. R. Fasham, Ed. (Springer, 2003) pp. 19-51.

18. J. T. Allen *et al.*, *Nature* **437**, 728 (2005).

19. I. Dadou, V. C. Garcon, V. Andersen, G. R. Flierl, C. S. Davis, *J. Mar. Res.* **54**, 311 (1996).

20. V. H. Strass, *Deep-Sea Res.* **39**, 75 (1992).

21. S. A. Spall, K. J. Richards, *Deep-Sea Res. I* **47**, 1261 (2000).

22. E. N. Sweeney, D. J. McGillicuddy, K. O. Buesseler, *Deep-Sea Res. II* **50**, 3017 (2003).

23. B. Mouriño Carbillido, D. J. McGillicuddy Jr., *Limnol. Oceanogr.* **51**, 2675 (2006).

24. R. R. Leben, G. H. Born, B. R. Engebreth, *Marine Geodesy* **25**, 3 (2002).

25. Materials and methods are available as supporting material on Science Online.

26. D. K. Steinberg *et al.*, *Deep-Sea Res. II* **48**, 1405 (2001).

27. A qualitatively similar feature was observed at BATS in April 2001 (BATS 150), during which time a cyclone of similar magnitude was present at the time series site.

28. We view this estimate as a lower bound on the implied remineralization, as this calculation ignores dilution of the oxygen deficit by mixing with waters outside the eddy core.

29. C. S. Davis, F. T. Thwaites, S. M. Gallager, Q. Hu, *Limnol. Oceanogr.: Methods* **3**, 59 (2005).

30. The small-scale (order 10km) fluorescence patchiness observed in the Video Plankton Recorder survey (Fig. 3A) is reminiscent of submesoscale frontal phenomena present in high-resolution numerical simulations (*14, 15, 19, 21*). Details of the relationship between, and interactions among, submesoscale and mesoscale processes remain a topic of active research. The key aspect of the observed fluorescence distribution as it pertains to diagnosis of the underlying mechanism (see below) is that the enhancement resides at eddy center, not at the periphery.

31. Picophytoplankton concentrations determined by flow cytometry showed no significant difference in standing stocks of *Prochlorococcus* spp. or *Synechococcus* spp. between A4 and C1, although their relative contribution to total chlorophyll a decreased significantly in A4 because of the large diatom bloom (Fig. 2B).

32. J. D. McNeil *et al.*, *J. Geophys. Res.* **104**, 15537 (1999).

33. Ironically, the basin-scale pattern of low biomass and productivity of the subtropical North Atlantic has been attributed to the presence of mode waters [J. B. Palter, M. S. Lozier, R. T. Barber, *Nature* **437**, 687 (2005)], yet our results illustrate how mesoscale lenses of this water can create the most intense plankton blooms ever observed in the region.

34. Depth integrated bacterioplankton biomass and production were not significantly different from the long-term mean at BATS. However, compared to C1,

volumetric bacterioplankton biomass and production in A4 were significantly enhanced within the deep chlorophyll a maximum where diatoms dominated.

35. J. C. Goldman, D. J. McGillicuddy Jr., *Limnol. Oceanogr.* **48**, 1176 (2003).

36. Spectoradiometric observations of photosynthetically available radiation (PAR) in eddy A4 indicated the depth of 1% of the surface value (a proxy for euphotic zone depth) had a mean of 96m (s.d. = 9 m, N = 37), nearly identical to that reported for BATS [D. A. Siegel et al., *Deep-Sea Res. II* **48**, 1865 (2001)]. Findings in C1 were similar, with a mean 1% PAR depth of 97 m (s.d. = 12 m, N = 49).

37. S. Levitus, in *NOAA Prof. Paper No. 13*. (U.S. Govt. Printing Office, Washington DC, 1982) pp. 173pp.

38. Altimetric data point toward the northern source region for the one year period during which the eddy could be tracked (Fig. 1B). However, initial analysis of radioisotope measurements offers conflicting evidence: radiocarbon data suggest a northern source, whereas tritium data suggest a southern source.

39. Nitrate to silicate ratios were similar in cyclone C1 and mode-water eddy A4. Concentrations in the upper euphotic zone were consistent with nitrogen limitation, as excess silicate (ca. 1-2 μmol kg^{-1}) was present in waters in which nitrate was depleted (< 0.1 μmol kg^{-1}). All of the eddies we studied exhibited a similar tendency for the phosphocline to reside deeper than the nitracline, leading to supra-Redfield nitrate:phosphate ratios just below the euphotic zone. This enigmatic aspect is characteristic of the region [A. F. Michaels et al., *Deep-Sea Res.* **41**, 1013 (1994); J. Wu, W. Sunda, E. A. Boyle, D. M. Karl, *Science* **289**,

759 (2000)]. Nevertheless, we could find no systematic differences in nitrate to phosphate ratios between cyclones and mode-water eddies.

40. A. P. Martin, K. J. Richards, *Deep-Sea Res. II* **48**, 757 (2001).

41. The Martin and Richards model predicts the vertical velocity at the base of the layer through which wind stress can be transmitted directly through waves and turbulence (the Ekman layer). Quasigeostrophic theory and models demonstrate that this vertical motion penetrates well into the inviscid interior, diminishing with depth [W. K. Dewar, G. R. Flierl, *J. Phys. Oceanogr.* **17**, 1653 (1987)]. We ran a primitive equation model simulation of eddy A4, which indicated that the vertical velocity at the depth of the high-chlorophyll layer is ca. 90% of the Ekman upwelling velocity. The physical manifestation of this effect is a tendency for upward displacement of the seasonal pycnocline at eddy center, enhancing the mode-water eddy structure (Fig 1A).

42. Note that this model also predicts upwelling in the interior of regular anticyclones. An analogous phenomena has been hypothesized to upwell depressed density surfaces in the interiors of warm-core Gulf Stream rings [W. K. Dewar, G. R. Flierl, *J. Phys. Oceanogr.* **17**, 1653 (1987)], a process that would tend to enhance biological activity associated with their frictional decay [P. J. S. Franks, J. S. Wroblewski, G. R. Flierl, *J. Geophys. Res.* **91**, 7603 (1986)].

43. D. M. Karl, E. A. Laws, P. Morris, P. J. l. B. Williams, S. Emerson, *Nature* **426**, 32 (2003).

44. A. Oschlies, *Global Biogeochem. Cycles* **16**, 1106 doi:10.1029/2001GB001830 (2002).

45. D. J. McGillicuddy, L. A. Anderson, S. C. Doney, M. E. Maltrud, *Global Biogeochem. Cycles* **17**, 1035 doi:10.1029/2002GB001987 (2003).

46. We thank the officers and crews of the R/V *Oceanus* and R/V *Weatherbird II* for their outstanding support during our seagoing operations. Dr. Robert Leben provided near-real-time altimetric data that was crucial for our adaptive sampling effort. Nutrient samples were processed by the Nutrient Analytical Facility (Paul Henderson) at WHOI. Numerical simulations were performed at NCAR's Scientific Computing Division. We thank Olga Kosnyreva for expert data analysis and visualization, and Sue Stasiowski for administrative support. We gratefully acknowledge the efforts of all participants in the EDDIES project, which included a number of BATS technicians. For more information see http://science.whoi.edu/users/olga/eddies/EDDIES_Project.html. The EDDIES project was funded by the National Science Foundation Chemical, Biological, and Physical Oceanography Programs. Additional support for remote sensing aspects (including altimetry and QuikSCAT wind analyses) and HPLC pigment assays (Dr. Charles Trees, CHORS) was provided by NASA.

Figure Legends

Fig. 1. (**A**) Isopycnal displacements associated with three types of eddies. Two density surfaces are depicted: one in the seasonal thermocline ρ_1, and one in the main thermocline ρ_2. Arrows indicate the sense of the vertical velocity arising from interaction of the wind with the underlying eddy-driven flow, which is upward in anticyclones and mode-water eddies and downward in cyclones. This eddy-wind interaction stimulates diatom blooms in mode-water eddies. (**B**) Objective analysis of sea level anomaly for 17 June 2005, just prior to the first cruise of the 2005 field season. The Gulf Stream mean path and meander envelope (one standard deviation) are indicated as solid and dashed black lines, respectively. Prior trajectories of the features of interest are indicated by white lines emanating from eddy centers, with dots at thirty day intervals. Satellite ground tracks are shown for Jason (magenta), Topex 2 (green), Geosat Follow-on (black), and ERS/ENVISAT (light blue). A corresponding map for the 2004 field season is provided in fig. S1.

Fig. 2. (**A**) Histogram of subsurface maxima in chlorophyll *a* from BATS data 1998-2003. Peak chlorophyll *a* values in cyclones (C1, C2, C3, C5) and mode-water eddies (A1, A4, A5) from the present observations (Table S1) are indicated by thin vertical lines. Inset: means of the peak chlorophyll *a* concentrations ($\mu g\ kg^{-1}$) in cyclones and mode-water eddies (MWEs) from the present observations, compared to the mean subsurface maximum at BATS. (**B**) Phytoplankton species composition (75-140m depth interval) in cyclone C1 (OC404-1 station 18) and mode-water eddy A4 (OC415-1 station

16). Estimates of the relative abundance (by pigment mass) of seven different groups, expressed as the percentage of total chlorophyll *a*, were calculated from HPLC pigment data together with the algorithms described in R. M. Letelier et al., *Limnology and Oceanography* **38**, 1420 (1993). Means and associated 95% confidence intervals for each group, derived from the BATS data for 1989-2003, are indicated in both plots. Lower panels: oxygen profiles in cyclone C1 (**C**) and mode-water eddy A4 (**D**). Envelope of BATS measurements 1988-2003 indicated by bold lines.

Fig. 3. (**A**) Three-dimensional distribution of chlorophyll *a* fluorescence (relative units) from VPR Survey of A4, overlayed on contours of sea level anomaly (mm) from objectively analyzed satellite data as in Fig. 2. (**B**) ^{14}C primary production profiles inside mode-water eddy A4, August 2005. Minimum, maximum and mean of BATS summertime observations from 1988-2003 are indicated by thick black lines.

Fig. 4. Winds and computed vertical velocities arising from wind-eddy interactions in cyclone C1 (top) and mode-water eddy A4 (bottom). Satellite-based wind measurements along the eddy trajectories (determined by satellite altimetry and shipboard observations) were obtained from QuikSCAT level 3 data, available on a 0.25° twice-daily global grid (see http://podaac.jpl.nasa.gov/quikscat/). Time periods of ship occupations by R/V *Oceanus* and R/V *Weatherbird II* are indicated by horizontal bars. Shipboard wind observations (R/V *Oceanus*) reveal excellent agreement with the satellite-based measurements. Vertical velocities at eddy center are computed using the formulae of

Martin and Richards (2001) assuming a spatially uniform wind over the eddy. Use of a spatially-variable wind introduces additional high-frequency fluctuations in vertical velocity, but their impact on the mean is less than 10%. Vertical velocity estimated from SF_6 tracer release in mode-water eddy A4 (0.4 m d^{-1}) for the time period between the release and the final survey is indicated by a dashed line in the lower panel.

Supporting Online Material

www.sciencemag.org
Materials and Methods
Figure S1
Tables S1, S2, S3

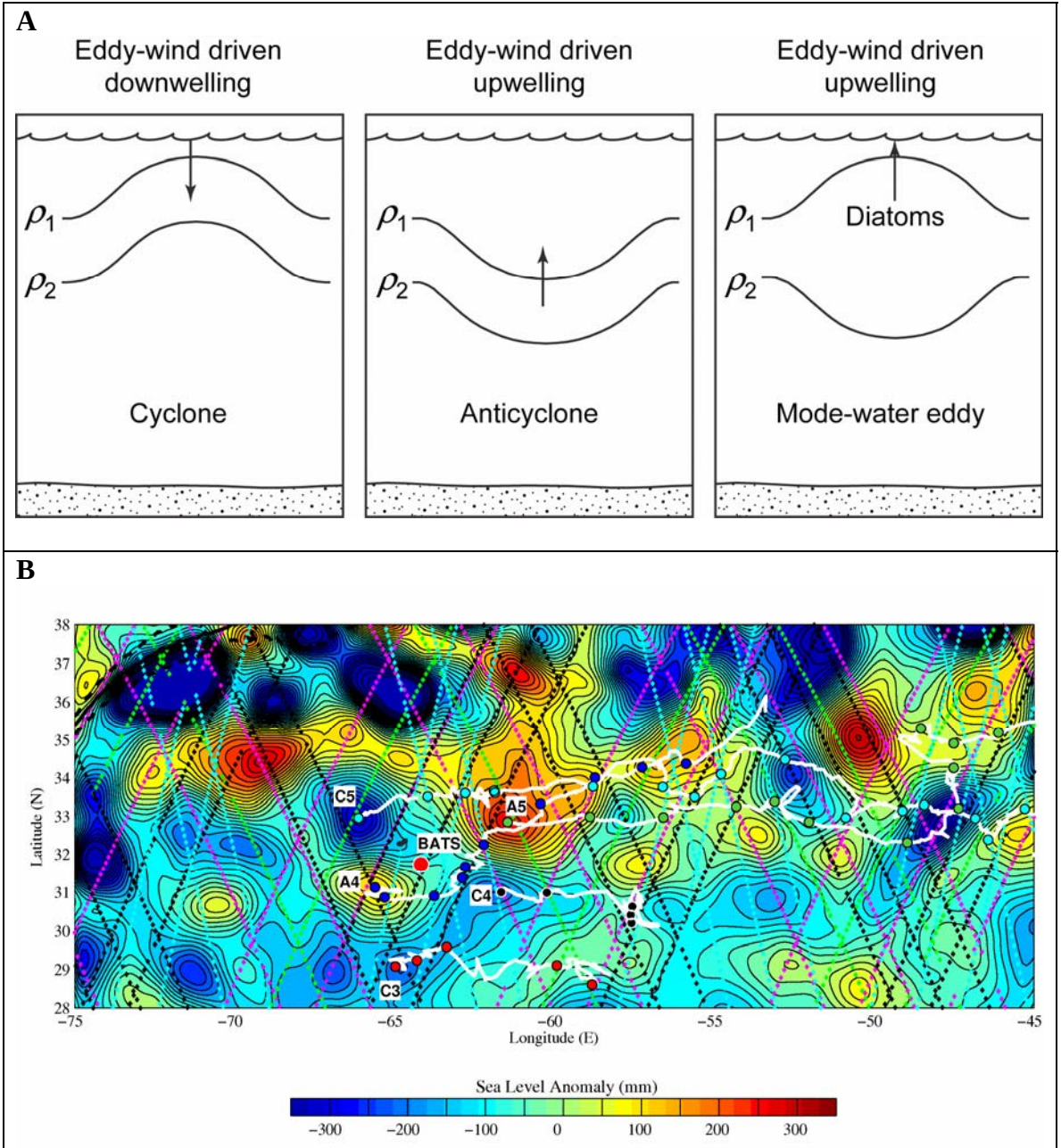

McGillicuddy et al., Fig. 1.

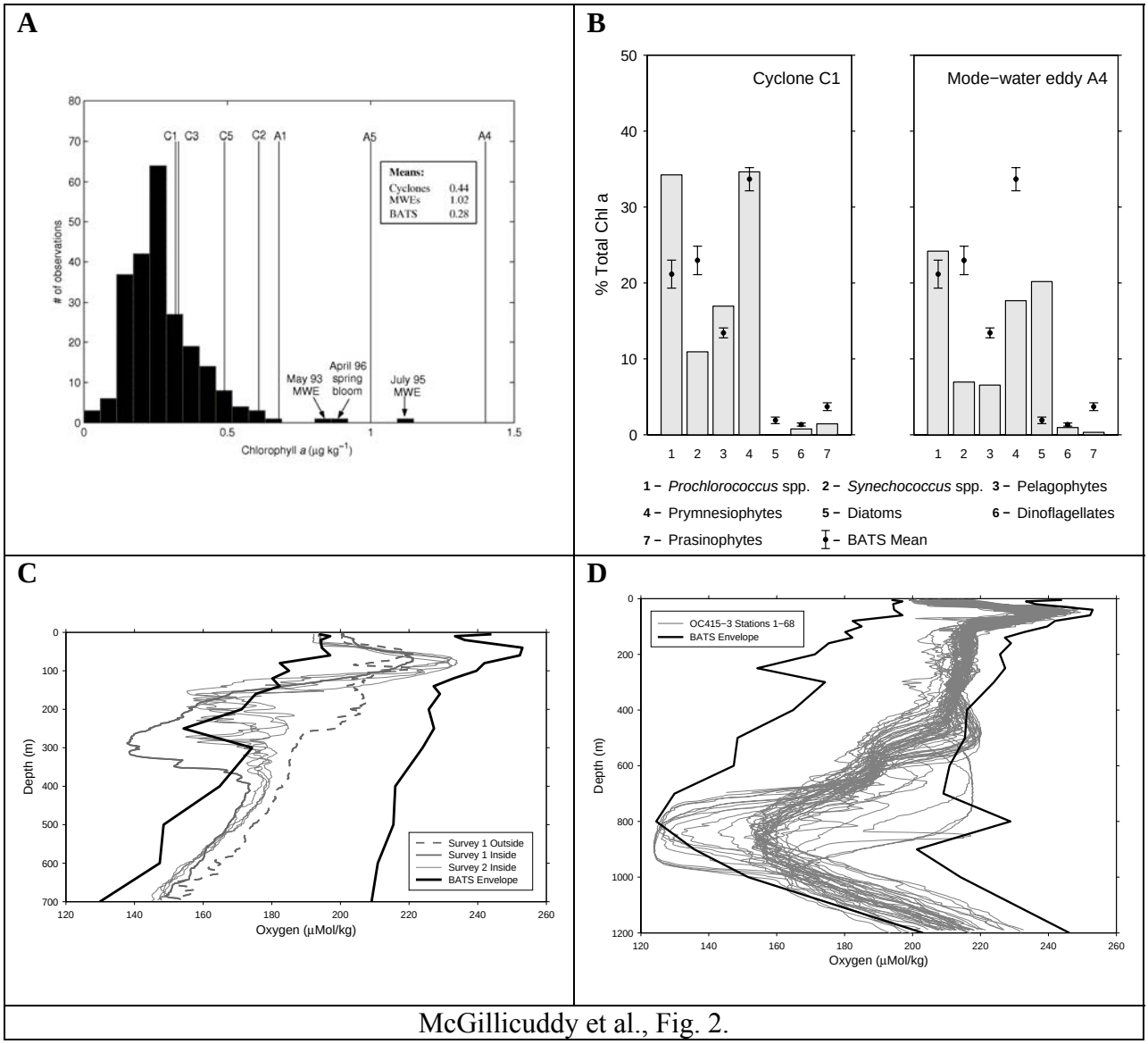

McGillicuddy et al., Fig. 2.

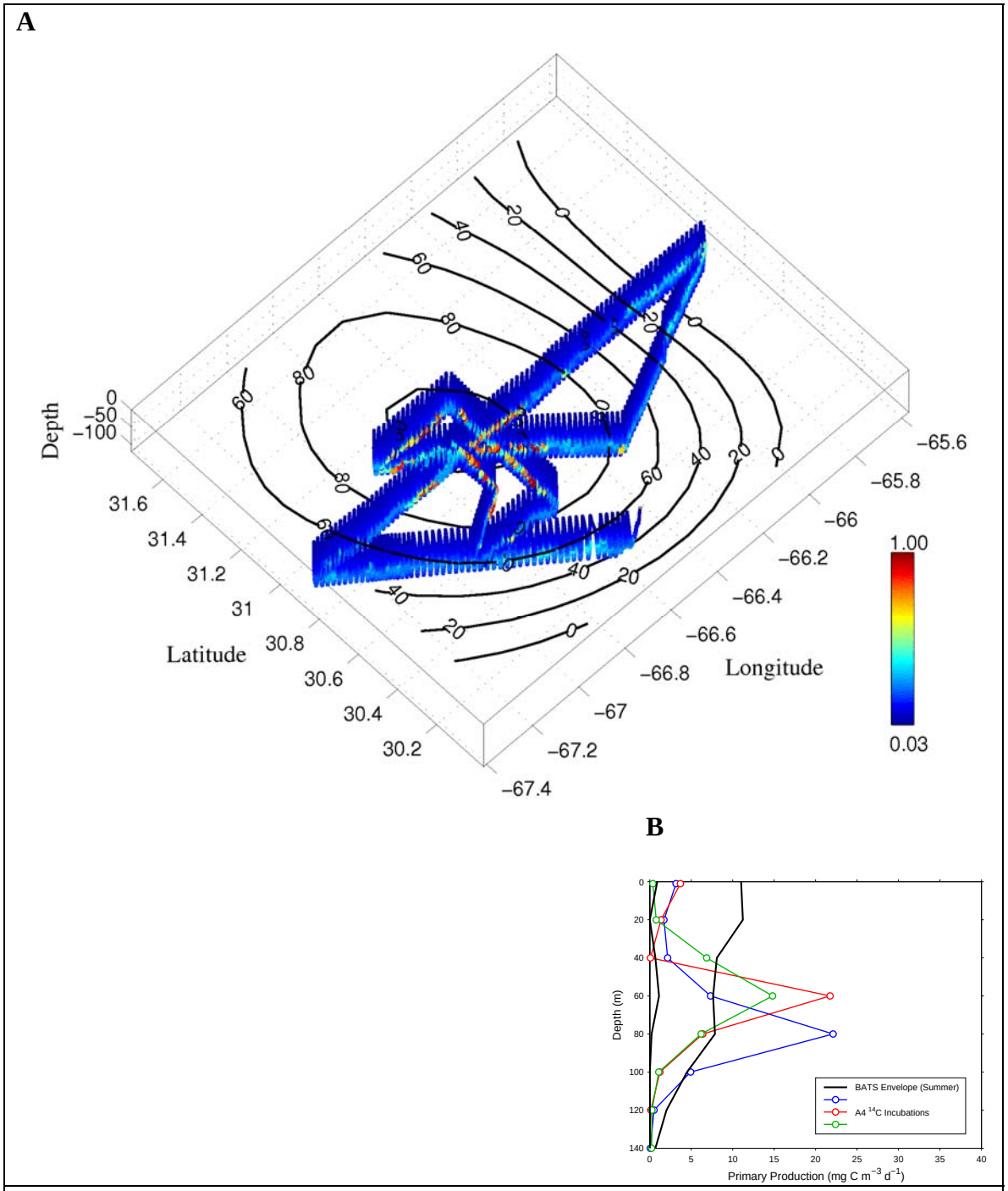

McGillicuddy et al., Fig. 3.

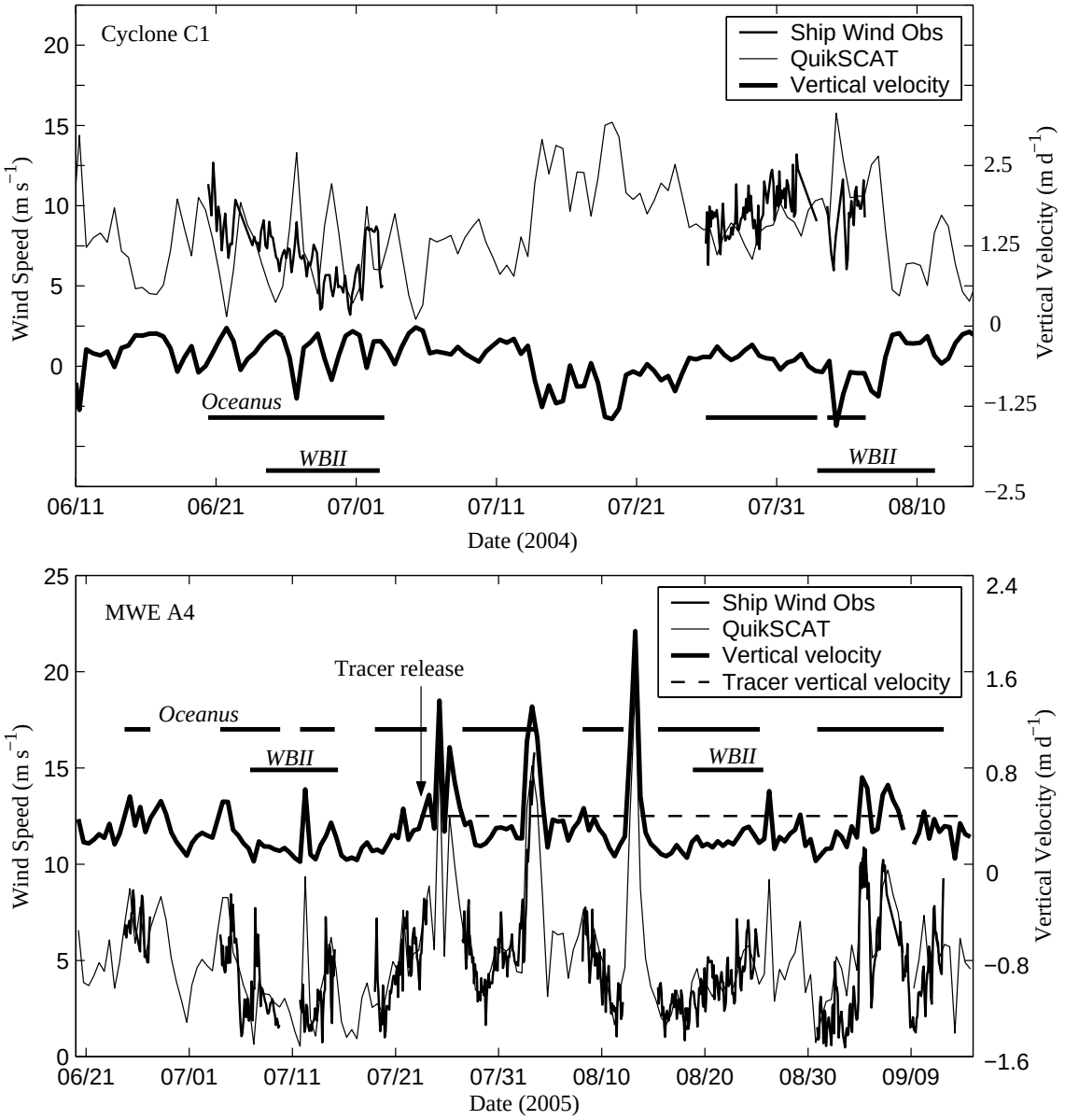

McGillicuddy et al., Fig. 4.

Supporting Online Material

Materials and Methods

All hydrographic measurements were made in accordance with the BATS protocols (*S1*) to insure compatibility between the two data sets. Nutrients were measured with a standard autoanalyzer, chlorophyll *a* with Turner extraction, and accessory pigments with HPLC. Dawn-to-dusk ^{14}C primary production incubations took place on drifting *in situ* arrays, and export flux was measured at 150m with drifting sediment traps (PITS). Methods for ^{234}Thorium-based flux estimates are described in (*S2*).

Bacterial production was measured using the incorporation of 3H-TdR by the microcentrifuge method (*S3*). Rates were converted to carbon using 1.63 x 10^{18} cells mol TdR^{-1} and 10 fg C $cell^{-1}$. Heterotrophic bacterial biomass was determined by counting DAPI-stained cells on a blackened 0.2μm PC filter via epifluorescence microscopy.

Zooplankton samples were collected with a 1 m^2 MOCNESS (EDDIES) and a standard 1 m^2 frame (BATS). The MOCNESS nets were 150 μm mesh compared with 200 μm mesh nets for the BATS time-series. The smallest size fraction was excluded from our samples and the BATS samples due to discrepancy in the net mesh size. Thus, the values reported here represent zooplankton >500 μm integrated from 0-150 m. We include nighttime tows only.

The tracer release consisted of 1.6 kg of sulfur hexafluoride (SF_6) injected on the 1026.26 kg m^{-3} potential density surface within 20km of eddy center, where the highest

chlorophyll *a* was found. Injection took place on July 23, 2005, and the tracer was tracked through September 11, 2005. Distribution of the tracer was measured with a vertical array of samplers (*S4*). The center of the array was held on a fixed isopycnal surface, while the array was towed at a speed of approximately 0.75 m s^{-1} for ten hours at a time. Fifty syringes at the center of the array filled sequentially along the tracks, 12 minutes being required to fill each syringe. Samples were analyzed on board ship with a gas chromatograph and electron capture detector by the head space technique (*S5*).

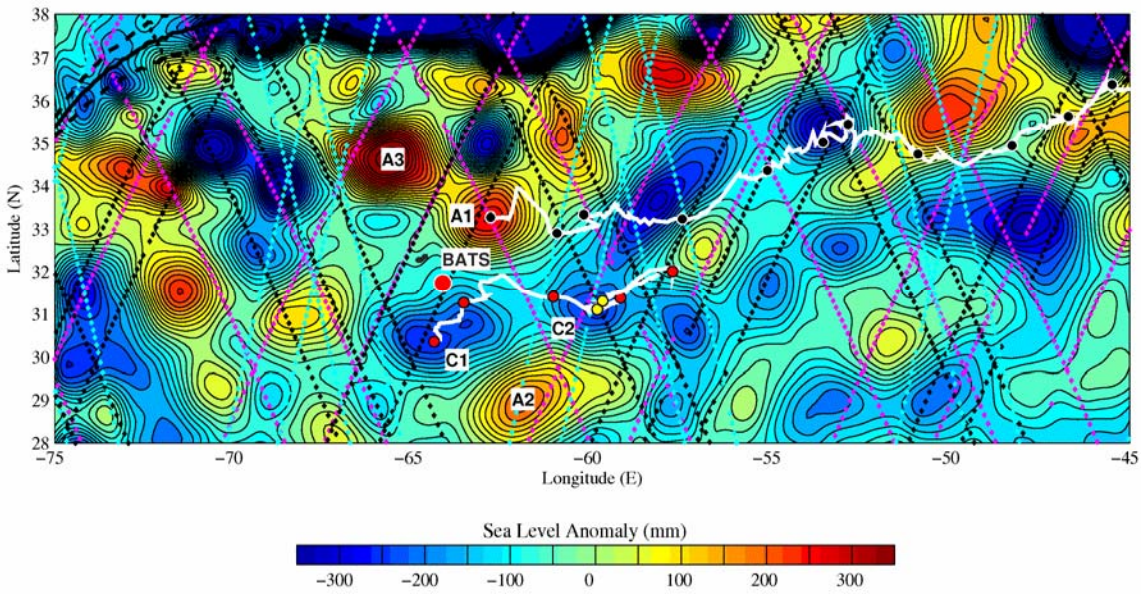

Fig. S1. Objective analysis of sea level anomaly for 5 June 2004, just prior to the first cruise of the 2004 field season. The Gulf Stream mean path and meander envelope (one standard deviation) are indicated as solid and dashed black lines, respectively. Prior trajectories of the features of interest are indicated by white lines emanating from eddy centers, with dots at thirty day intervals. Satellite ground tracks are shown for Jason (magenta), Topex 2 (green), Geosat Follow-on (black), and ERS/ENVISAT (light blue).

Eddy type	Feature	Occupations	Cruises
Cyclones	C1	4	OC404-1/WBIIX0409 (3), OC404-4/WBIIX0413 (1)
	C2	2	OC404-1, OC404-4
	Cold-core ring	1	OC404-4
	C3	1	OC415-1
	C5	2	OC415-1
Regular	A2	1	OC404-1 (XBT/ADCP/VPR only)
Anticyclones	A3	1	OC404-1 (XBT/ADCP/VPR only)
Mode-water eddies	A4 (18°)	6	OC415-1/WBII X0506 (2), OC415-2, OC415-3/WBIIX0508 (2), OC415-4
	A1 (16°)	1	OC404-1
	A5 (16°)	2	OC415-1, OC415-3

Table S1. EDDIES Observations. Cruise dates were: OC404-1, June 11-July 3, 2004; WBII X0409, June 24-July 3, 2004; OC404-4: July 25-August 12, 2004; WBII X0413: August 3-12, 2004; OC415-1: June 20-July 15, 2005; WBII X0506: July 6-15, 2005; OC415-2: July 18-August 5, 2005; OC415-3: August 7-26, 2005; WBII X0508: August 17-26, 2005; OC415-4: August 29-September 15, 2005.

Eddy type	Date	Reference
Cyclones	January1993	S6
	July 1993	S6
	November 1993	S6
	August 1994	S6
	June 1996	S7
	June 1996	S7
	July 1997	Unpublished
Regular	March 1994	S6
Anticyclones	September 1994	S6
	June 1996	S7
Mode-water	May 1993	S6
eddies	July 1995	S6,S8
	October 1995	S6
	June 1995	S7

Table S2. Observations of eddies in the vicinity of the Bermuda Atlantic Time-series Study.

		Primary Production mg C m^{-2} d^{-1}	Bacterial Production mg C m^{-2} d^{-1}	Bacterial Biomass mg C m^{-2}	Zooplankton Biomass mg dry wt m^{-2}	^{234}Th-based Carbon flux mg C m^{-2} d^{-1}	Sediment Trap Flux mg m^{-2} d^{-1}		
							Mass	Carbon	Nitrogen
Cyclone C1									
	June-July 2004	403±119	24.0±4.3	725±110	328±163 535[1]	48±17	65.3	19.3	2.7
	August 2004	594	21.4±5.1	783±83	378±14 503±40[1]	20±8	68.1	23.0	3.5
MWE A4									
	July 2005	273±63	15.7±3.1	671±76	550±124	15±5	71.1±14.3	15.9±1.8	2.4±.28
	August 2005	688±107	21.8±3.0	579±84	515±305	22±9	63.5±6.4	12.4±.14	2.1±.14
BATS Summer Climatology		426±207 (1988-2003)	37.5±25 (1999-2002)	714±131 (1993-2003)	398±215 (1994-2005) 190±46 (2004-2005)		107.8±39.0	27.2±8.0	4.3±1.5

Table S3. Vertically integrated primary production (^{14}C incubation, 0-140m), bacterial production and biomass (TdR, DAPI, 0-140m), zooplankton biomass (0-150m, net tows), thorium-based carbon flux estimates, and sediment trap fluxes (150m, PITS) measured in target features C1 and A4, as compared with climatological summertime conditions at BATS. Mean values are reported with ±1 standard deviation. See Knap et al. (1993) for details on methodology. Zooplankton biomass (>500μm, in dry weight) integrated in over the upper 0-150m (nighttime tows only) in order to compare with the BATS zooplankton time-series. The smallest size fraction was removed from both EDDIES and BATS samples to accommodate discrepancy in the net mesh size. Notes: (1) denotes stations at eddy periphery.

Supporting Online Material: References

S1. A. H. Knap *et al.*, *BATS Methods Manual* (U.S. JGOFS Planning Office, Woods Hole, MA, 1993).

S2. K. O. Buesseler et al., *Limnol. Oceanogr.* **50**, 311 (2005).

S3. D. C. Smith, F. Azam, *Marine Microbial Food Webs* **6**, 107 (1992).

S4. J. R. Ledwell, A. J. Watson, C. S. Law, *J. Geophys. Res.* **103**, 21499 (1998).

S5. R. Wanninkhof, J. R. Ledwell, A. J. Watson, *J. Geophys. Res.* **96**, 8733 (1991).

S6. E. N. Sweeney, D. J. McGillicuddy, K. O. Buesseler, *Deep-Sea Res. II* **50**, 3017 (2003).

S7. D. J. McGillicuddy *et al.*, *J. Geophys. Res.* **104**, 13381 (1999).

S8. J. D. McNeil *et al.*, *J. Geophys. Res.* **104**, 15537 (1999).